European Journal of Pharmaceutics and Biopharmaceutics 140 (2019) 11–19

Contents lists available at ScienceDirect

European Journal of Pharmaceutics and Biopharmaceutics

journal homepage: www.elsevier.com/locate/ejpb

Research paper

Infrared spectroscopic study of the coil-helix transition of highly concentrated gelatin formulations

Fabian Polyak, Gabriele Reich*

University of Heidelberg, IPMB, Department of Pharmaceutical Technology and Biopharmaceutics, Im Neuenheimer Feld 329, 69120 Heidelberg, Germany

ARTICLE INFO

Keywords:
Gelatin
FTIR spectroscopy
Multivariate data analysis
Coil-helix transition
Gel elasticity
Hard gelatin capsules
Soft gelatin capsules

ABSTRACT

The aim of this study was to investigate the applicability of ATR-FTIR spectroscopy as an analytical tool to monitor the gel formation of highly concentrated gelatin formulations. Spectral changes induced by the coil-helix transition have been studied and related to the elasticity parameter G′ obtained by oscillatory rheology in simultaneous measurements. A principal component analysis of the amide I band allowed the evaluation of triple helix formation kinetics. It was found that the key frequencies of the amide I band at 1657 and 1612 cm^{-1} represent the transition of the gelatin molecules from the random coil to the triple helical conformation in the emerging gel. A direct correlation between the conformation of the gelatin molecules and the gel elasticity was obtained for a commercially available pharmaceutical grade limed bone gelatin in concentrations between 20 and 40% w/w. The same was valid upon addition of small gelatin peptides or a helix inhibitor. No such correlation between triple helix content and G′ was found for limed bone gelatins of the same Bloom value but an asymmetric molecular weight distribution with extremely high fractions of high or low molecular weight components. This suggests that early gel elasticity is not solely linked to the triple helix nucleation. Hence, our results indicate that FTIR spectroscopy can be applied to gain a better understanding of the relationship between triple helix content and elastic gel properties of pharmaceutical gelatin capsule shell formulations.

1. Introduction

Gelatin is a widely used and versatile pharmaceutical excipient known for its unique gelling properties. Pharmaceutical applications such as hard and soft capsules require gelatin concentrations > 20%. Both, hard and soft capsule manufacture rely on the thermo-reversible sol to gel transition associated with the unique structure of gelatin. Furthermore, the properties of the gel network are crucial for the machinability and the performance of the final product [1].

Gelatin is a protein obtained from the hydrolytic degradation of collagen, the major structural protein found in mammalian connective tissue. Upon hydrolysis the three-stranded and triple helical tropocollagen is decomposed into gelatin molecules with a broad distribution of random chain lengths. Commercially available gelatin is composed of monomers (α-chains), its cross-linked dimers (β-chains) and trimers (γ-chains) as well as smaller sub-units of the α-chain and higher molecular fragments of multiple connected strands, the so-called microgel fraction [2–4].

In native collagen, the right-handed triple helix is formed by three individual and closely packed α-chains stabilised by interchain hydrogen bonds. Each single chain has a well-defined left-handed helical structure due to the specific amino acid pattern found in most collagen types. Every third position in the α-chain is occupied by the amino acid glycine, generating an $(Gly\text{-}X\text{-}Y)_n$ repeating sequence. In mammalian gelatins, the imino acids account for approximately 25% of the residue composition [5]. Proline is found in X- and Y-position, whereas 4-hydroxyproline is exclusively located in the Y-position. Interchain hydrogen bonds between an amide C═O of the residues in X-position and −NH of glycine are crucial for the triple helix stability in collagen and gelatin [6].

Unlike cross-linked collagen fibrils, gelatin is soluble in water at elevated temperature. In aqueous solution gelatin exists in random coil conformation. Upon cooling a coil-helix transition occurs leading to a fully thermo-reversible gel at concentrations above 2%. Even though the exact mechanism of the physical gelation is still under investigation, it certainly involves the nucleation of two or three gelatin chains and a partial recovery of the collagen-like triple helical structure leading to junction zones between individual chains [7–9]. At the same time, β-turns allow the polypeptide chains to form intramolecular loops leading to an intramolecular nucleation [10]. After the initial nucleation step, the helix formation proceeds and an ‘infinite long’ ageing period of helix optimization and growth follows [11].

* Corresponding author.
E-mail address: gabriele.reich@uni-hd.de (G. Reich).

https://doi.org/10.1016/j.ejpb.2019.04.010
Received 28 December 2018; Received in revised form 5 April 2019; Accepted 12 April 2019
Available online 16 April 2019
0939-6411/

The gelation of aqueous gelatin solutions has been intensively studied with several experimental methods, including optical rotation [11], rheology [12] and differential scanning calorimetry (DSC) [13]. To investigate the mechanism and kinetics of the coil-helix transition, both the macroscopic gelation and the helix formation on the molecular level have to be assessed in combination. Papers published by Eldridge and Ferry proposed a model which related the elasticity of gelatin gels to physical cross-links between the gelatin molecules [14,15]. Since then, their approach to compare gel rheology with optical rotation measurements has been used by many investigators. The gel elasticity, represented by the storage modulus G′, has been widely used as an easily accessible mechanical parameter to monitor the gel formation [12,16–18]. Optical rotation measurements and DSC have been applied to determine the conformational changes and the helix fraction of gelatin gels [4,11,18,19]. It is well accepted that the gel formation kinetics and the gel structure strongly depend on the total content of triple helical junction zones and their growth as a function of temperature and time [9]. Up to now most experiments to investigate the coil-helix transition have been performed at low gelatin concentrations in the range between 0.5 and 15% w/w. Correlation between physical and chemical attributes of aqueous gelatin samples usually stems from data acquired in separate experiments. The thermal history of the samples is, however, of utmost importance since temperature is the main parameter affecting the structural and the viscoelastic properties of a gelatin gel.

A huge number of additional factors has been identified that directly affect the gelation properties of gelatin gels. These comprise the gelatin concentration, the molecular weight distribution, the solution pH, the electrolyte concentration or the addition of plasticizers, e.g. polyols [8,20,21].

Mid-infrared spectroscopy has first been used by Milch in the 1960's to monitor temperature-dependent changes of gelatin in D_2O [22]. Payne and Veis [23] and later Prystupa and Donald [24] studied gelatin/H_2O systems at different temperatures using ATR-FTIR (Attenuated Total Reflection Fourier-Transform Infrared Spectroscopy) and deconvolution techniques. These authors heavily relied on the amide I band to investigate the temperature-dependent conformational changes based on the hydrogen-bonding pattern of the gelatin molecules in concentrations < 12% w/w.

Until now there is a lack of an easy to use spectroscopic method to monitor the conformational changes during gelation of highly concentrated gelatin solutions > 20% w/w. Hence, the aim of this study was to investigate the applicability of ATR-FTIR spectroscopy as an analytical tool to detect the conformational changes of gelatin molecules from the random coil to the triple helical state. Simultaneous rheological measurements enabled us to relate the gel formation to the conformational transition and thus to improve the understanding of the relationship between the coil-helix transition and the mechanical properties of highly concentrated pharmaceutical gelatin formulations.

2. Materials and methods

We used three well-characterized 260 Bloom limed bone (LB) gelatins of different viscosity (GELITA AG, Germany). The gelatins were labeled according to their specified viscosity, measured in 6.67% w/w at 60 °C: medium (MV), high (HV) and low viscous (LV). The gelatin MV represents a commercial pharmaceutical grade limed bone quality with a high percentage of α-chains. The characteristics of the gelatins as provided by the supplier are listed in Table 1. The molecular weight distribution (MWD), the average molecular weight (MW) and the polydispersity index (PDI) were determined by a standardized gel permeation chromatography method with UV detection at 214 nm. Calibration of the GPC system was performed with a mixture of collagen standards including defined collagen fragments.

2.1. Sample preparation

Four sample sets of aqueous formulations containing 20–40% w/w gelatin in distilled water were prepared using a 3-h standardized melting, homogenization and degassing procedure. The first sample set was composed of 20–40% w/w gelatin MV in H_2O or 99.9% D_2O (Sigma Aldrich, Germany). For the second set, a non-gelling gelatin hydrolysate (Fortigel® from GELITA AG, Germany) with an average molecular weight of 3 kDa was added to samples containing 20 and 30% w/w gelatin MV to maintain the protein concentration at a constant level of 40% w/w. In the third set, 40% w/w gelatin MV was dissolved in either a 0.1 M NaSCN, a 0.2 M NaSCN solution or a 0.2 M sorbitol solution. The final sample set included the gelatins LV and HV at 40% w/w in water. A 40% w/w sample of the non-gelling gelatin hydrolysate in distilled water was used for comparison.

2.2. ATR-FTIR and rheological measurements

All spectral and rheological data were measured simultaneously on a HAAKE MARS III oscillatory rheometer with the Rheonaut module coupled to a Nicolet 6700 FTIR spectrometer (Thermo Scientific, Germany). An ATR crystal (diamond, single reflection) in the lower part of the plate/plate geometry allowed recording the spectra in the centre of the sample. The diameter of the upper plate was 35 mm and the gap size was 1 mm. The rim of the gelatin samples was covered with liquid paraffin to avoid dehydration of the sample. The built-in peltier controlled heating device allowed temperature steps of 0.1 °C. A linear cooling ramp from 70 to 25 °C with a temperature gradient of 0.5 °C/min was applied, followed by a 90 min isothermal ageing period at 25 °C. The IR spectra were recorded in one-minute intervals with 24 scans at 4 wavenumber resolution. The rheometer was operated in controlled shear deformation mode with 1% deformation and a frequency of 1 Hz, while recording the shear stress amplitude. The dynamic viscoelastic functions, namely the storage modulus G′ and the loss modulus G″ were determined as a function of temperature.

2.3. Data processing

In each run, a set of 180 spectra was recorded. The relevant structural information was obtained from the amide I band using the wavenumbers from 1695 to 1592 cm^{-1}. Multivariate data analysis utilizing principal component analysis (PCA) was applied to highlight the substantial spectral changes [25]. A PCA was performed with The Unscrambler® X (Camo Software AS, Norway) software version 10.4 using the NIPALS algorithm with and without mean centring of the data set. The resulting score line plots of the first or second principal component (PC-1 or PC-2) were used to determine the coil-helix transition. The average of five score line plots from repeated measurements was taken for our investigation. To equalize the different data acquisition

Table 1
Characteristics of the gelatins. MWD data were determined by gel permeation chromatography.

	Bloom (g)	**Viscosity** (mPa·s)	**MW** (g/mol)	**PDI**	**Sub-units** (%)	**Alpha** (%)	**Beta** (%)	**Gamma** (%)	**Microgel** (%)
Gelatin MV	260	4.61	145 386	2.29	26.37	35.92	17.47	15.28	4.96
Gelatin LV	259	2.78	93 441	2.41	47.73	30.56	13.90	6.35	1.46
Gelatin HV	258	8.55	231 050	2.47	14.17	26.54	17.17	20.13	21.99

geometries in the sample gap, the scores were raised to the power of 1.5. For the ease of interpretation, all averaged score line plots were transformed to match the alignment of the G′ curve and normalized to the reference formulation containing 40% w/w gelatin MV in distilled water. The transformed score line plots are denoted as score ratio plots.

2.4. Differential scanning calorimetry

DSC measurements (n = 3) were performed using a Mettler Toledo DSC 822 system (Mettler Toledo, Germany). Closed aluminum crucibles were filled with 20 ± 2 mg of the same samples as applied to the rheometer. To imitate the thermal procedure of the rheometer setup, a DSC protocol with a linear cooling ramp from 70 to 25 °C and a temperature gradient of 5 °C/min followed by a 90 min isothermic ageing period at 25 °C was performed. The melting enthalpy was calculated from the final heating step from −25 to 75 °C at a rate of 5 °C/min and is given in J/g sample weight. For a better comparison with the multivariate spectroscopic data, the enthalpy values are also given as percentage relative to the 40% w/w gelatin MV reference sample.

3. Results and discussion

3.1. Spectral analysis of the amide I band

Fig. 1a shows the FTIR spectra of a 40% w/w solution of gelatin MV and distilled water at 25 °C in the range of 1800–1000 cm^{-1}. The broad overlap of the amide I band, caused by the strong IR absorbance of water molecules (O—H—O bending mode around 1640 cm^{-1}) demonstrates the great challenge of the spectroscopic analysis of measurements with a continuously changing temperature. One often used strategy to overcome the disturbance caused by the solvent is the subtraction of the solvent spectrum from the sample spectra and the subsequent use of band narrowing techniques like Fourier self-deconvolution (FSD) or second derivative spectra to enhance the resolution of the peptide absorption bands [23,24,26,27]. Such an approach was not appropriate for our continuous analysis with a constant cooling rate from 70 to 25 °C. Instead, we have chosen a multivariate approach utilizing a principal component analysis (PCA) of the amide I band from 1695 to 1592 cm^{-1} to highlight the gelatin absorbance and to find the key frequencies relevant for the conformational transition of the repeating Gly-X-Y sequence. The PCA revealed a change of the spectral absorption of the sample as a function of temperature, visible in the score line plot of the first principal component PC-1 (Fig. 1b).

We found that the spectral change described by the score line plot of PC-1 was in close accordance with the simultaneously measured storage modulus G′, shown as dashed line in Fig. 1b. The storage modulus G′ described the sol to gel transition on the macroscopic scale as an increase of the elasticity in the emerging gel upon cooling, whereas the spectroscopic response in the score line plot allowed to simultaneously determine the underlying conformational changes of the gelatin molecules. We transformed the score line plot as described in Section 2.3 to further highlight the interrelation of both curves in the temperature range of the sol to gel transition (Fig. 1d). In the cooling phase, the resulting plots of the storage modulus and the scores of the first principal component were congruent. In the following isothermal gel-ageing phase at 25 °C a slight shift of the score ratio plot from the G′ profile appeared. This shift is caused by the residual influence of the solvent on the PCA calculation.

The first principal component contains all the information about the temperature-dependent conformational transition of the gelatin molecules as well as at least most of the non-linear temperature influence of water, representing > 95% of the variance of the amide I peak. To better separate the relevant information of the conformational transition of the gelatin backbone from the interfering solvent effects, we performed the PCA calculation without mean centring the data set. The information of the conformational change is then represented by the second principal component, whereas the aforementioned residual solvent effects remain in the first principal component (Fig. 1e + f).

Actually, the enhanced accuracy gained by the second principal component is accompanied by the fact that PC-2 describes only a small part of the overall spectral variance. Both calculation procedures reliably extract the spectral information related to the conformational transition of the gelatin molecules. The choice of the calculation method therefore depends on the specific requirements of the application.

According to the loadings plot, the main contributing wavenumbers are 1612, 1657 and to a lower extent 1681 cm^{-1} (Fig. 1c + e). The loadings plot illustrates the frequencies with the most distinct intensity changes of the amide I band as calculated for each principal component. These frequencies can be attributed to the amide carbonyls of the gelatin molecules that undergo the most prominent change of hydrogen bonding upon gelation. The time evolution of the raw spectra at the corresponding frequencies are shown in Fig. 2. Both bands, 1657 and 1612 cm^{-1} show a similar time-dependent progress as the associated score line plot. There is no significant change in the intensity of both frequencies in the sol state, while both frequencies undergo a rapid change below 38 °C. The intensity of the 1612 cm^{-1} peak decreases in the same way as the intensity at 1657 cm^{-1} increases. Measurements of pure water as well as a non-gelling gelatin hydrolysate revealed no distinctive alteration in both, the raw spectra and the PCA of the amide I band.

The amide I peak of gelatin has its origin in the C═O stretching vibrational mode of the amide bond of the polypeptide backbone. Any conformational change of the gelatin molecules such as the coil-helix transition is thus reflected in the spectra. A great number of peak frequencies in the amide I and II bands of globular proteins have already been identified and assigned to common protein structures such as α-helix, β-sheets, β-turns and others [26,28,29]. Considering the unique Gly-X-Y amino acid sequence of gelatin with its high content of proline and hydroxyproline, it is unlikely to find these common motifs in a gelatin gel. Instead, we expect the triple helices of gelatin to dominate the amide I peak. Upon gelation the individual gelatin chains in the sol develop junction zones of collagen-like triple helical structures, which act as physical links in the growing gel network. Interchain hydrogen bonds comparable to those found in collagen are stabilising these triple helical regions.

Throughout the coil to helix transition, the amide carbonyls participating in the interchain hydrogen bonds replace their bonding partner from −OH of a water molecule to −NH of glycine on an adjacent chain [30]. In the special case of an intrachain helix next to a β-turn, the −NH donating glycine is located on the same gelatin molecule. Thus, the most distinctive frequencies found in the loadings plot can be attributed to the hydrogen bonds at the triple helical nucleation sites. The inverse time course of the peaks at 1657 and 1612 cm^{-1} implies that both frequencies are related to the same amide carbonyl in the X-position of the gelatin triplet structure.

Our assignments are in good accordance with the frequencies found in a FTIR study performed by Prystupa and Donald [24] on lower concentrated gelatin samples. The authors were able to resolve the fine structure of the amide I peak by deconvolution and curve fitting of gelatin samples in the sol and the gel state. They interpreted 1613 cm^{-1} as hydrogen bonds between the carbonyl of the imino acids in the gelatin chain and solvent water molecules. The band at 1659 cm^{-1} was assigned to helical structures and β-turns, matching our results from the PCA.

The loadings plot exhibits two further peaks that are less related to the sol to gel transition. The peak frequency at 1681 cm^{-1} and the more shoulder-like peak at 1632 cm^{-1} are of noticeably less intensity and do not change in the same temperature-dependent manner as 1657 and 1612 cm^{-1}. Prystupa and Donald assigned the frequencies 1681 and 1629 cm^{-1} to β-turns and to solvent imino acid hydrogen bonds and possibly β-sheets. However, to our knowledge, no solid proof for the

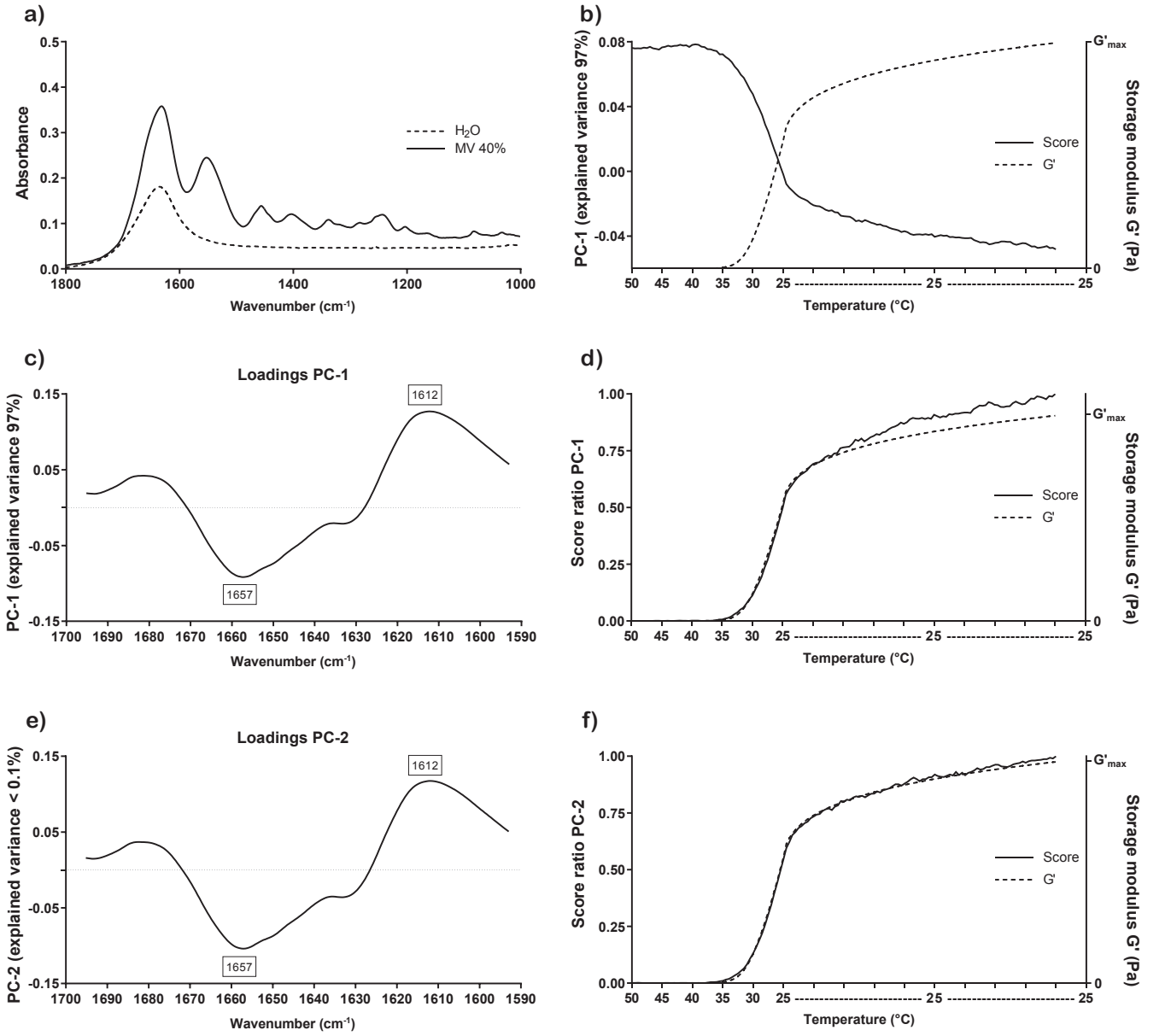

Fig. 1. FTIR spectra of a 40% w/w solution of gelatin MV and distilled water at 25 °C (a). The storage modulus G′ of the 40% w/w sample of gelatin MV and the associated score line plot (b), the loadings plot (c) and the score ratio plot (d) of the first principle component PC-1. The loadings plot (e) and the score ratio plot (f) of the second principal component PC-2 of the same sample.

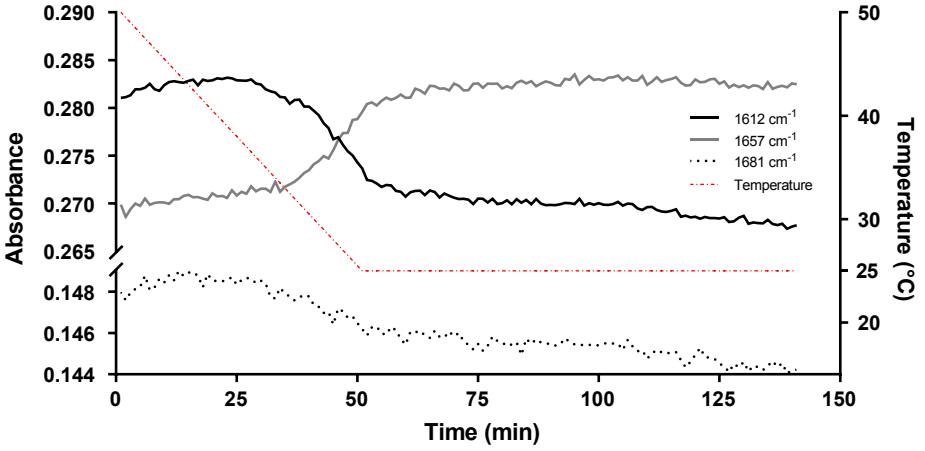

Fig. 2. The time course of the three most prominent amide I peak frequencies found in the loadings plot. The graph shows the peak signal transition of the raw spectra. The red dashed line indicates the sample temperature. (For interpretation of the references to color in this figure legend, the reader is referred to the web version of this article.)

occurrence of ß-sheets in gelatin has been published yet. The peak at 1632 cm^{-1} is located very close to the OH bending vibration mode around 1635 cm^{-1}, the prominent spectral feature of water in the amide I region.

To investigate and exclude the potential spectral interference of water, we conducted an experiment with the same gelatin in D_2O, which shows no absorption in the amide I region. The resulting peak frequencies in the loadings plot were comparable to the aqueous sample, including the peak near 1632 cm^{-1}. The key frequencies attributed to the triple helix formation remained the main features and shifted from 1657 cm^{-1} and 1612 cm^{-1} in H_2O to 1649 cm^{-1} and 1616 cm^{-1} in D_2O. The secondary peak frequencies were found with slight shifts in the D_2O loadings plots, confirming the gelatin as their origin. Overall, PCA revealed at least two peak frequencies in the amide I peak which can be precisely assigned to the triple helix formation.

3.2. Relationship between spectral features and triple helix content

To evaluate the potential application of this multivariate IR approach in the development and production of hard and soft gelatin capsules, we performed three series of experiments. We used gelatin MV and varied the triple helix content in different ways, namely by (1) varying the gelatin concentration between 20 and 40% w/w, (2) replacing part of the gelatin by non-gelling gelatin hydrolysate, and (3) adding a helix promoter or inhibitor. Simultaneous spectroscopic and rheological measurements enabled the spectral changes to be related to both, the triple helix content and the increase in gel elasticity.

As expected, samples containing a lower amount of gelatin (< 40% w/w) revealed a decrease in their storage modulus G′ due to a reduced number of triple helical junction zones in the gel network (Fig. 3). Likewise, the spectral change in the amide I peak decreased according to the score ratio plots. However, the lower amount of gelatin molecules in the sample leads to a lower absorbance of the amide carbonyls. This in turn has an impact on the signal intensity ratio between gelatin and water, i.e. at lower gelatin concentrations the score ratio plot calculated by the conventional PCA was more susceptible to spectral noise and more important to OH bending motions of the solvent. In our experimental setup, the perturbation from water was twofold, first the OH bending peak masked the key frequencies of the conformational transition of the gelatin molecules and second the peak additionally experienced an inherent temperature-dependent shift [31]. At gelatin concentrations < 30% w/w, the spectral influence from the water molecules progressively dominated the outcome of the PCA thus limiting this approach to samples with a high gelatin to water ratio. In the case of gelatin concentrations lower than 15% w/w, the scores and loadings of the first principal component mainly represented the temperature-dependent spectral shift of the OH bending peak. By utilizing the PCA calculation with the non-centred spectral data set, this interference could be successfully decreased. This approach enabled us to reliably expand the detection limit for the coil-helix transition to gelatin concentrations below 20% w/w.

To vary the triple helix content without reducing the absorbance of the amide I band, we replaced some of the gelatin MV in the samples by a non-gelling gelatin hydrolysate. This allowed the number of amide bonds in the formulation to be maintained at the same level, which in turn excludes concentration-dependent effects on the PCA calculation. Fig. 4a shows the score ratio plots and the storage moduli of the gelatin samples with 10 and 20% w/w of gelatin being replaced by the non-gelling hydrolysate. The storage modulus G′ decreased for the samples with the lower gelatin MV content due to the lower amount of triple helices in the gel network. Differences in the triple helix content were also reflected in the score ratio plots, indicating less conformational transition in the amide I band of the spectra upon addition of the hydrolysate.

The results reveal the complex kinetics of triple helix formation, as the probability of nucleation upon cooling is very sensitive to the concentration of gelatin molecules in the sample. Triple helix formation of the 40% w/w gelatin MV sample without hydrolysate (G40%/H0%) started at a higher temperature compared to the G30%/H10% and G20%/H20% samples (Fig. 4a), since the longer gelatin chains are closest to each other without any disturbance by the small hydrolysate molecules. Substitution of gelatin MV by gelatin hydrolysate decreased the storage modulus and the score ratio, indicating a lower triple helix formation. These results confirm the concentration dependency of the gelation mechanism, as the probability of nucleation events increases with higher concentrations. The kinetics of the helix growth in the isothermal part of the gelation were found to be less concentration-dependent, as all the score ratio plots were found to run nearly in parallel. Similar findings were reported for optical rotation experiments with lower concentrated gelatin samples [32].

The differences in G′ and the score ratio between the pure gelatin MV sample and the samples containing hydrolysate indicate a stabilising effect of the non-gelling hydrolysate on the gel formation that cannot be solely explained by the viscosity increase. Since the small peptide molecules of the hydrolysate retain their ability to form short triple helices [30], we assume that the interaction with the longer gelatin molecules helps to establish or stabilise triple helix nucleation.

To vary the triple helix content without varying the concentration of the gelatin MV molecules in the sample, we added either a promoter or inhibitor of helix nucleation to samples of 40% w/w gelatin MV. Sorbitol is known to stabilise helix nucleation and subsequent growth, leading to a greater helix fraction in the gel [13,20]. On the contrary, the addition of NaSCN and other salts can inhibit the gelation if present in sufficient concentrations [21]. The opposing effects of sorbitol and NaSCN are shown in Fig. 4b.

The addition of 0.2 M sorbitol increased the storage modulus as well as the associated score ratio, whereas the addition of 0.1 M NaSCN led to a decrease in both G′ and the conformational transition indicated in the score ratio plot. The inhibition of the helix formation was even more pronounced upon addition of 0.2 M NaSCN. Both additives seem to directly affect the triple helix formation as G′ and the score ratio plots were equally altered. Interestingly, the gelation temperature was less affected, as only the addition of 0.2 M NaSCN significantly altered the gelation kinetics.

Complementary DSC measurements provided further evidence that the scores from the PCA represent the formation of triple helices. The melting enthalpy of gelatin gels has been related to the loss of hydrogen bonds that stabilise the triple helix [33] and hence used as a measure of the degree of triple helix formation [19]. For our samples, the melting enthalpy values obtained by DSC were found to be proportional to the score ratio at the end of the isothermic phase. With the 40% w/w sample of gelatin MV set as the reference, the ratio of the melting enthalpies from DSC and the ratio from the score plots were found to be comparable (Table 2). The decrease in the melting enthalpy of the samples containing gelatin hydrolysate was in line with the decline of the score ratios for each formulation. A similar correlation was found for the samples with modified helix nucleation.

Overall, the results indicate that the course of the score plots is almost exclusively driven by the conformational change of the gelatin molecules from their random coil structure in the sol state to the collagen-like triple helical network in the gel state.

3.3. Impact of the molecular weight distribution on the conformational transition

Contrary to the previous findings, we did not find a direct correlation between the spectroscopic signal and G′ for the gelatin types HV and LV. Both gelatin types differ from average commercial gelatin qualities due to their unusual asymmetric molecular composition (Fig. 5). In case of gelatin HV the increase of G′ started at a higher temperature and reached a higher maximum value compared to gelatin MV as indicated in Fig. 6. According to the score ratio plots the helix

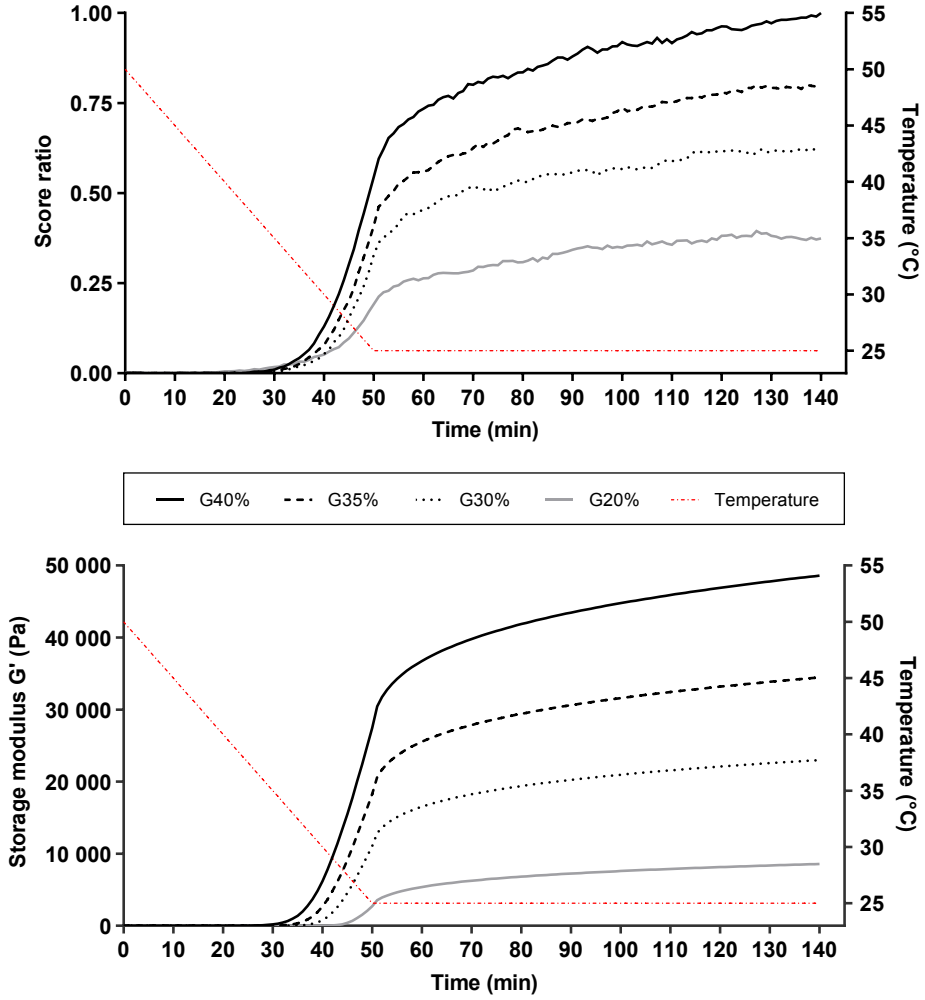

Fig. 3. Score ratio plots of the second principle component of gelatin MV samples from 20 to 40% w/w upon cooling (top). The corresponding storage moduli G′ of the same samples (bottom). The red dashed line indicates the sample temperature. (G: gelatin). (For interpretation of the references to color in this figure legend, the reader is referred to the web version of this article.)

formation was, however, noticeably decreased. Moreover, the kinetics of helix formation and gel elasticity were not concurrent. Gelatin type LV was found to behave in the opposite way, with a higher amount of helix formation compared to gelatin MV accompanied by lower G′ values. Likewise helix formation and gel elasticity did not start at the same temperature; in case of gelatin LV the increase of G′ was delayed compared to the helix formation.

Both, the structural and the rheological properties of a gelatin gel strongly depend on the molecular weight distribution of the gelatin, which directly results from the gelatin source and the extraction process [32]. In general, manufacturers of pharmaceutical LB gelatin supply their products as blends with a more or less symmetric molecular weight distribution around the α-chain fraction, thus comprising only low amounts of the very small sub-units < 18 000 g/mol and the microgel fraction > 400 000 g/mol.

Gelatin HV is, however, dominated by the large covalently cross-linked collagen fragments of the microgel leading to the high viscosity of this gelatin. We assume that on average the microgel has less flexibility to reform triple helical structures compared to the smaller single chain fragments. This is due to the greater steric constraints of the covalent cross-links. In our highly concentrated 40% w/w samples, the rigid and bulky structure of these large covalently cross-linked molecules contributes to the mechanical elasticity mainly by enhanced entanglements. This overcompensates the reduced helix formation of that fraction at the early gelation stage and explains the increase in G′ prior to the detection of helix nucleation.

On the contrary, the low-viscous gelatin LV is mainly composed of molecules smaller than the α-chain and nearly lacking the microgel fraction. Compared to the gelatin MV, the gelatin LV comprises significantly less covalently linked molecules and hence requires more intermolecular triple helical nucleation sites to form a gel network of comparable elasticity. The prevalence of sub-units of the α-chain increase the incidence of intramolecular helix formation, explaining the increased detection of triple helical structures accompanied by a lower gel elasticity. Hence, a direct correlation between G′ and the spectroscopic variance of the amide I band is not valid for all gelatin types and grades.

In addition to the data presented in this paper, we have investigated a wide range of commercial gelatin grades, including pigskin, limed hide and limed bone gelatins of Bloom values ranging from 100 to 300 Bloom. From these studies, it has been obvious that triple helix formation and gel formation are not necessarily concurrent, as only interchain nucleation contributes notably to the gel network. If early helix formation mostly occurs within a single chain or these early nucleation sequences are less stable due to less chain entanglements, the conformational change does not necessarily need to accompany network formation. Both, LV and HV are rare examples of gelatin grades with an asymmetric, i.e. non-standard molecular weight distribution and thus do not represent the majority of pharmaceutical gelatins used in hard and soft capsule manufacture.

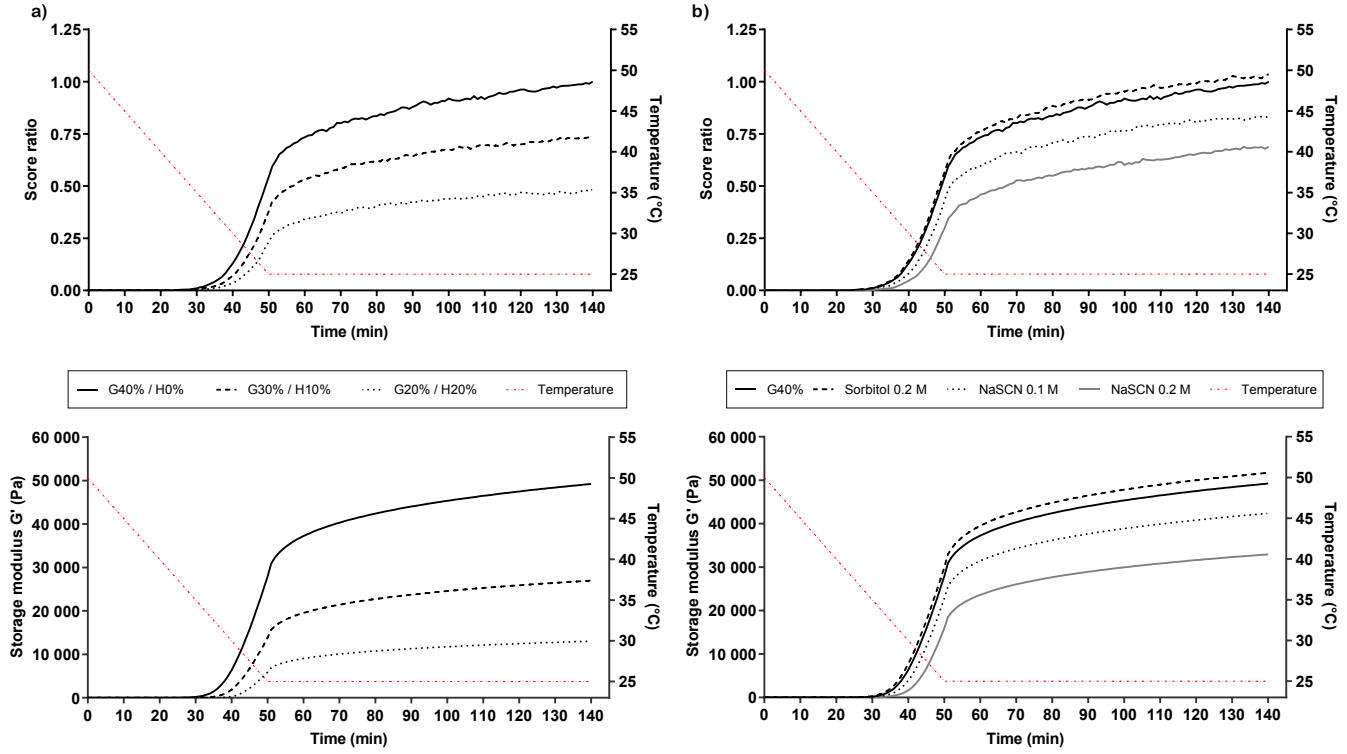

Fig. 4. Score ratio plots of the first principle component (top) and the respective storage moduli (bottom) of gelatin MV samples with the addition of a non-gelling gelatin hydrolysate (a) and sorbitol or NaSCN (b) at different concentrations. The red dashed line indicates the sample temperature. (G: gelatin; H: hydrolysate). (For interpretation of the references to color in this figure legend, the reader is referred to the web version of this article.)

Table 2
Comparison between the melting enthalpy (DSC) and the score ratio (FTIR) of gelatin MV at different concentrations with and without additives. The 40% w/w sample without additives was set as the reference.

Gelatin conc. (% w/w)	**Additive**	**Conc. of additive**	**Melting enthalpy** (J/g)	**Score ratio**	**Enthalpy** (%)	**Score ratio** (%)
40	–	–	4.78 ± 0.05	1	100.0	100.0
35	–	–	4.03 ± 0.08	0.804	84.3	80.4
30	–	–	3.15 ± 0.08	0.625	65.8	62.5
30	Hydrolysate	10%	3.73 ± 0.06	0.732	78.0	73.2
20	Hydrolysate	20%	2.25 ± 0.04	0.480	47.1	48.0
40	Sorbitol	0.2 M	4.93 ± 0.01	1.034	103.2	103.4
40	NaSCN	0.2 M	3.40 ± 0.13	0.688	71.1	68.8
40	NaSCN	0.1 M	3.97 ± 0.01	0.832	83.1	83.2

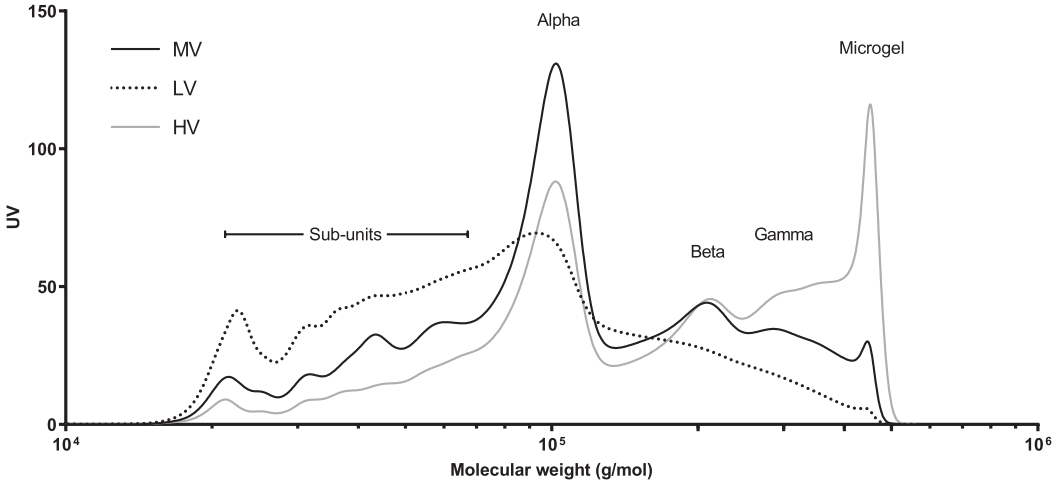

Fig. 5. The molecular weight distribution of the limed bone gelatins MV, LV and HV obtained by gel permeation chromatography.

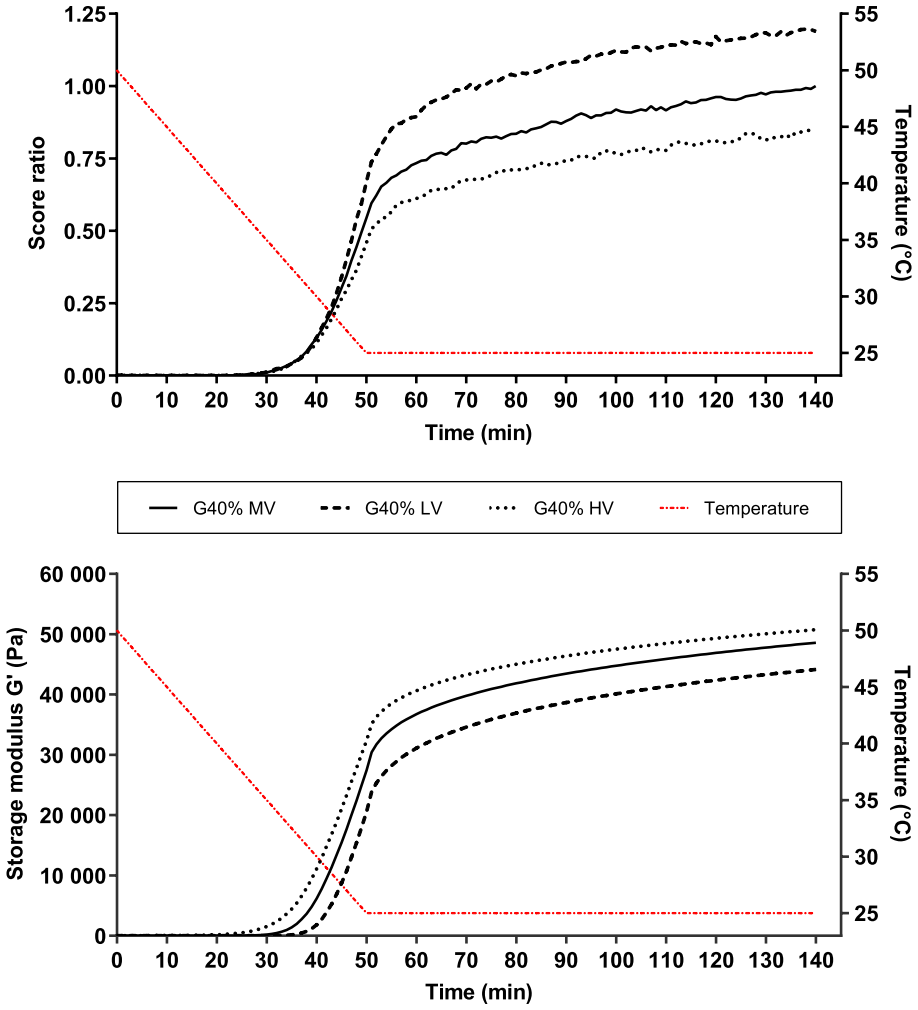

Fig. 6. Score ratio plots of the second principle component (top) and the respective storage moduli (bottom) of the gelatin samples MV, LV and HV. The red dashed line indicates the sample temperature. (G: gelatin). (For interpretation of the references to color in this figure legend, the reader is referred to the web version of this article.)

4. Conclusions

The results of our study show that ATR-FTIR spectroscopy is an efficient analytical tool to monitor the triple helix formation in highly concentrated gelatin formulations. Utilizing the multivariate PCA approach, we have succeeded to observe the temperature- and formulation-dependent spectral changes during the gelation process. Decomposition of the spectral changes of the amide I band enabled to discriminate the conformation of the gelatin molecules in the sol and the gel state. According to our findings, the amide I band of gelatin gives rise to two major peak frequencies at 1657 and 1612 cm^{-1} representing the triple helix formation during the sol to gel transition. The loadings plot allowed to assign these frequencies to the formation of hydrogen bonds during triple helix nucleation and the following helix growth. With this approach it was possible to correlate the triple helix formation of a commercially available pharmaceutical limed bone gelatin with the increase in gel elasticity. However, experiments with limed bone gelatin grades comprising an unusual asymmetric molecular weight distribution with extremely high amounts of either small or large components suggest that early gel elasticity is not solely linked to the triple helix formation.

Overall, our approach can be applied to gain a better understanding of the relationship between triple helix content and elastic gel properties and thus provides a reliable and robust spectroscopic method to monitor the gelation process of pharmaceutical gelatins. We see strong potential in the development and manufacture of gelatin based pharmaceutical products such as soft and hard capsules.

Acknowledgements

The authors want to thank Dr. Wilfried Babel for many fruitful discussions and comments on the manuscript.

References

[1] G. Reich, Formulation and physical properties of soft capsules, in: F. Podczeck, B. Jones (Eds.), Pharm. Capsul. Pharmaceutical Press, London, 2004, pp. 201–212.
[2] F.A. Johnston-Banks, Gelatine, in: P. Harris (Ed.), Food Gels, Springer, Netherlands, Dordrecht, 1990, pp. 233–289, , https://doi.org/10.1007/978-94-009-0755-3_7.
[3] W. Babel, Gelatine - ein vielseitiges Biopolymer, Chemie Unserer Zeit. 30 (1996) 86–95, https://doi.org/10.1002/ciuz.19960300205.
[4] S.B. Ross-Murphy, Structure and rheology of gelatin gels: recent progress, Polymer (Guildf). 33 (1992) 2622–2627, https://doi.org/10.1016/0032-3861(92)91146-S.
[5] M.D. Shoulders, R.T. Raines, Collagen structure and stability, Annu. Rev. Biochem. (2009), https://doi.org/10.1146/annurev.biochem.77.032207.120833.
[6] J. Bella, M. Eaton, B. Brodsky, H. Berman, Crystal and molecular structure of a collagen-like peptide at 1.9 A resolution, Science 266 (1994) 75–81, https://doi.org/10.1126/science.7695699.
[7] A. Veis, The Macromolecular Chemistry of Gelatin, Academic Press, New York, 1964.
[8] A.G. Ward, A. Courts (Eds.), The Science and Technology of Gelatin, Academic Press, London, 1977.
[9] M. Djabourov, Gelation—A review, Polym. Int. (1991), https://doi.org/10.1002/pi.4990250302.
[10] J.P. Busnel, E.R. Morris, S.B. Ross-Murphy, Interpretation of the renaturation

kinetics of gelatin solutions, Int. J. Biol. Macromol. (1989), https://doi.org/10.1016/0141-8130(89)90053-6.
[11] M. Djabourov, J. Leblond, P. Papon, Gelation of aqueous gelatin solutions. I. Structural investigation, J. Phys. (1988), https://doi.org/10.1051/jphys:01988004902031900.
[12] K. te Nijenhuis, Investigation into the ageing process in gels of gelatin/water systems by the measurement of their dynamic moduli - Part I: phenomenology, Colloid Polym. Sci. 259 (1981) 522–535, https://doi.org/10.1007/BF01397890.
[13] G. Reich, Effect of sorbitol specification on structure and properties of soft gelatin capsules, Pharm. Ind. 58 (1996) 941–946.
[14] M. Miller, J.D. Ferry, F.W. Schremp, J.E. Eldridge, Studies of the cross-linking process in gelatin gels. II: static rigidity and stress relaxation, J. Phys. Colloid Chem. 55 (1951) 1387–1400, https://doi.org/10.1021/j150491a014.
[15] J.E. Eldridge, J.D. Ferry, Studies of the cross-linking process in gelatin gels. III. Dependence of melting point on concentration and molecular weight, J. Phys. Chem. 58 (1954) 992–995, https://doi.org/10.1021/j150521a013.
[16] K. te Nijenhuis, Investigation into the ageing process in gels of gelatin/water systems by the measurement of their dynamic moduli - Part II: mechanism of the ageing process, Colloid Polym. Sci. 259 (1981) 1017–1026, https://doi.org/10.1007/BF01558616.
[17] J. Peyrelasse, M. Lamarque, J.P. Habas, N. El, Bounia, Rheology of gelatin solutions at the sol-gel transition, Phys. Rev. E - Stat. Phys., Plasmas, Fluids, Relat. Interdiscip. Top. 53 (1996) 6126–6133, https://doi.org/10.1103/PhysRevE.53.6126.
[18] L. Guo, R.H. Colby, C.P. Lusignan, A.M. Howe, Physical gelation of gelatin studied with rheo-optics, Macromolecules (2003), https://doi.org/10.1021/ma034266c.
[19] J.L. Gornall, E.M. Terentjev, Helix-coil transition of gelatin: Helical morphology and stability, Soft Matter. (2008), https://doi.org/10.1039/b713075a.
[20] D. Oakenfull, A. Scott, Stabilization of gelatin gels by sugars and polyols, Top Catal. (1986), https://doi.org/10.1016/S0268-005X(86)80018-2.
[21] G. Reich, Actions and optimization of plasticizers in soft gelatin capsules, Pharm. Ind. 58 (1994) 915–920.
[22] R.A. Milch, Infra-red spectra of deuterated gelatin sols, Nature 202 (1964) 84–85, https://doi.org/10.1038/202084a0.
[23] K.J. Payne, A. Veis, Fourier transform ir spectroscopy of collagen and gelatin solutions: deconvolution of the amide I band for conformational studies, Biopolymers (1988), https://doi.org/10.1002/bip.360271105.
[24] D.A. Prystupa, A.M. Donald, Infrared study of gelatin conformations in the gel and sol states, Polym. Gels Netw. 4 (1996) 87–110, https://doi.org/10.1016/0966-7822(96)00003-2.
[25] G. Reich, Near-infrared spectroscopy and imaging: Basic principles and pharmaceutical applications, Adv. Drug Deliv. Rev. 57 (2005) 1109–1143, https://doi.org/10.1016/J.ADDR.2005.01.020.
[26] D.M. Byler, H. Susi, Examination of the secondary structure of proteins by deconvolved FTIR spectra, Biopolymers (1986), https://doi.org/10.1002/bip.360250307.
[27] G. Reich, Mid and near infrared spectroscopy, in: A. Müllertz, Y. Perrie, T. Rades (Eds.), Anal. Tech. Pharm. Sci. Springer, New York, NY, 2016, pp. 61–138, , https://doi.org/10.1007/978-1-4939-4029-5_3.
[28] A. Barth, Infrared spectroscopy of proteins, Biochim. Biophys. Acta - Bioenerg. (2007), https://doi.org/10.1016/j.bbabio.2007.06.004.
[29] M. Carbonaro, A. Nucara, Secondary structure of food proteins by Fourier transform spectroscopy in the mid-infrared region, Amino Acids 38 (2010) 679–690, https://doi.org/10.1007/s00726-009-0274-3.
[30] Y.A. Lazarev, B.A. Grishkovsky, T.B. Khromova, Amide I band of IR spectrum and structure of collagen and related polypeptides, Biopolymers (1985), https://doi.org/10.1002/bip.360240804.
[31] Y. Maréchal, Infrared spectra of water. I. Effect of temperature and of H/D isotopic dilution, J. Chem. Phys. 95 (1991) 5565–5573, https://doi.org/10.1063/1.461630.
[32] N. Elharfaoui, M. Djabourov, W. Babel, Molecular weight influence on gelatin gels: structure, enthalpy and rheology, Macromol. Symp. (2007) 149–157, https://doi.org/10.1002/masy.200751017.
[33] P.L. Privalov, E.I. Tiktopulo, Thermal conformational transformation of tropocollagen. I. Calorimetric study, Biopolymers (1970), https://doi.org/10.1002/bip.1970.360090202.